JAS 1099

Tracking Rigid Body Motion Using Thrusters and Momentum Wheels

Christopher D. Hall*, Panagiotis Tsiotras†, and Haijun Shen‡

Abstract

Tracking control laws are developed for a rigid spacecraft using both thrusters and momentum wheels. The model studied comprises a rigid body with external thrusters and with rigid axisymmetric wheels controlled by axial torques. Modified Rodrigues parameters (MRPs) are used to describe the kinematics. The thruster torques and the axial motor torques are computed to track given attitude motions, using the angular velocity error and MRP error to develop linear and nonlinear control laws. Three different controllers are developed. The first controller uses thruster torques based on a bang-bang control law, while momentum wheels are used to correct tracking errors.

* Associate Professor, Department of Aerospace and Ocean Engineering, Virginia Polytechnic Institute and State University, Blacksburg, Virginia, 24061. Phone: (540) 231-2314, email: cdhall@vt.edu

† Associate Professor, School of Aerospace Engineering, Georgia Institute of Technology, Atlanta, Georgia 30332. Phone: (404) 894-9526, email: p.tsiotras@aerospace.gatech.edu

‡ Ph.D. Candidate, School of Aerospace Engineering, Georgia Institute of Technology, Atlanta, Georgia 30332. Phone: (404)894-6302, email: haijun_shen@ae.gatech.edu

The second controller is similar, but is designed to use the thruster torques in such a way that the momentum wheels are not used at all unless there are initial condition errors. The third controller uses linear feedback for the wheels and nonlinear feedback for the thrusters. In all three cases, the controllers are shown rigorously to result in globally asymptotically stable closed-loop systems.

Introduction

The problem of reorienting a satellite has been studied by numerous authors, and much of the relevant material is contained in the monograph by Junkins and Turner [1]. Many researchers have considered only external torques, such as would be provided by thrusters or magnetic torquers; Ref. [2] gives a detailed literature review, and develops external torque control laws similar to those developed herein. Internal torques are also used in many spacecraft, both for attitude control, and for rotational maneuvers; Ref. [3] gives references and develops simple control laws for large-angle rotational maneuvers. In Ref. [4], we applied a similar approach to the problem of simultaneous energy storage and attitude control using flywheels.

In some highly maneuverable spacecraft, one may consider incorporating both thrusters and momentum wheels as attitude control actuators. Thrusters typically provide higher control authority than momentum wheels, and hence are useful for providing the torque for rapid reorientation maneuvers. However, thrusters typically do not have fine-resolution throttling capability and are therefore not as useful for precision control. Another disadvantage of thrusters is their dependence on expend-

able propellant. Momentum wheels have lower control authority, but are capable of finer control, and have the distinct advantage of using electrical energy. However, to achieve large torques with momentum wheels requires large angular accelerations which in turn requires high power. When large torques are required and thrusters are not admissible (for example, to avoid plume impingement or exhaust accumulation on sensitive optics), control moment gyros are typically used. However, in non-sensitive applications, the combination of thrusters and momentum wheels could be a valuable alternative to expensive control moment gyros. These arguments indicate that the combination of thrusters and momentum wheels might be effective for spacecraft that occasionally perform large-angle maneuvers and that have fine pointing requirements. The thrusters would provide the primary maneuver torque, while the momentum wheels provide the fine control to remove initial condition errors.

In this paper, we develop three different controllers that incorporate both internal and external torques. These controllers are logical extensions to the controllers developed in Ref. [2], and are shown to render the complete system dynamics and kinematics globally asymptotically stable. We begin by establishing the system model and appropriate rotational equations of motion. We also introduce a virtual reference frame whose motion the spacecraft attitude is required to track. The attitude motion of the virtual reference frame is due to a reference torque, which is computed offline and used as a feedforward element in the control laws. The rotational kinematics are described using Modified Rodrigues Parameters (MRPs) [5]. We introduce a Lya-

punov function which has been previously introduced in Ref. [2] and also used in Ref. [6]. The Lyapunov function is used to establish the stability of the three controllers, which each allocate the thruster and momentum wheel control differently. We illustrate the effectiveness of the controllers with a series of numerical examples.

System Model

We consider a rigid spacecraft $\mathcal{B}$ with N rigid and axisymmetric, balanced momentum wheels, $\mathcal{W}_i,\ i = 1, \cdots, N$, and three thrusters capable of providing torques about the principal axes. Let $\mathbf{N}$ denote the inertial frame, and $\mathbf{B}$ denote a body frame with origin at the center of mass of the system $\mathcal{B} + \sum_{i=1}^{N} \mathcal{W}_i$. The desired trajectory to be tracked is generated by a "virtual" spacecraft with the same inertia properties as the rigid spacecraft. Let $\mathbf{R}$ denote the reference frame which is fixed at the center of mass of this virtual spacecraft.

The purpose of the controller is to make the body frame $\mathbf{B}$ asymptotically track the reference frame $\mathbf{R}$. In addition, in the absence of any disturbances and any errors in the initial conditions, the tracking controller should keep $\mathbf{B}$ and $\mathbf{R}$ aligned at all times.

Dynamics

Let $\mathbf{I}$ be the moment of inertia of the system, including the wheels and thrusters, and let $\mathrm{I}_{si}, i = 1, 2, \cdots, N$ denote the axial moments of inertia of the momentum wheels. Defining the matrix $\mathbf{I}_s = \mathrm{diag}\{\mathrm{I}_{s1}, \cdots, \mathrm{I}_{sN}\}$, we have the dynamics of the

system described by [1]

$$\dot{\mathbf{h}}_B = \mathbf{h}_B^{\times}\mathbf{J}^{-1}(\mathbf{h}_B - \mathbf{A}\mathbf{h}_a) + \mathbf{g}_e \tag{1}$$

$$\dot{\mathbf{h}}_a = \mathbf{g}_a \tag{2}$$

where $\mathbf{h}_B$ is the system angular momentum vector in frame $\mathbf{B}$ given by

$$\mathbf{h}_B = \mathbf{I}\boldsymbol{\omega}_B + \mathbf{A}\mathbf{I}_s\boldsymbol{\omega}_s \tag{3}$$

In Eqs. (1–3), $\mathbf{h}_a$ is the $N \times 1$ matrix of the *axial* angular momenta of the wheels, $\mathbf{g}_e$ is the 3×1 matrix of external torques applied by the thrusters, $\mathbf{g}_a$ is the $N \times 1$ matrix of the internal axial torques applied by the platform to the momentum wheels, $\mathbf{A}$ is the $3 \times N$ matrix containing the axial unit vectors of the N momentum wheels, and $\mathbf{J}$ is a positive definite, inertia-like matrix defined as

$$\mathbf{J} = \mathbf{I} - \mathbf{A}\mathbf{I}_s\mathbf{A}^T \tag{4}$$

From Eqs. (3) and (4) the angular velocity of frame $\mathbf{B}$ can be written as

$$\boldsymbol{\omega}_B = \mathbf{J}^{-1}(\mathbf{h}_B - \mathbf{A}\mathbf{h}_a) \tag{5}$$

and the *axial* angular momenta of the momentum wheels can be written as

$$\mathbf{h}_a = \mathbf{I}_s\mathbf{A}^T\boldsymbol{\omega}_B + \mathbf{I}_s\boldsymbol{\omega}_s \tag{6}$$

where $\boldsymbol{\omega}_s = (\omega_{s1}, \omega_{s2}, \cdots, \omega_{sN})^T$ is an $N \times 1$ vector denoting the axial angular velocities of the momentum wheels with respect to the body.

Kinematics

Modified Rodrigues Parameters (MRPs) [5] are used to describe the kinematics of the attitude motion. The MRPs are defined as

$$\boldsymbol{\sigma} = \hat{\mathbf{e}} \tan(\Phi/4) \tag{7}$$

where $\hat{\mathbf{e}}$ is the unit vector along the Euler principal axis, and Φ is the Euler principal rotation angle [2]. The differential equations of the kinematics in terms of the MRPs are

$$\dot{\boldsymbol{\sigma}} = \mathbf{G}(\boldsymbol{\sigma})\boldsymbol{\omega} \tag{8}$$

where

$$\mathbf{G}(\boldsymbol{\sigma}) = \frac{1}{2}\left(\mathbf{1} + \boldsymbol{\sigma}^{\times} + \boldsymbol{\sigma}\boldsymbol{\sigma}^{T} - \frac{1+\boldsymbol{\sigma}^{T}\boldsymbol{\sigma}}{2}\mathbf{1}\right) \tag{9}$$

and $\mathbf{1}$ is the 3×3 identity matrix. Therefore, the kinematics of the body frame can be written as

$$\dot{\boldsymbol{\sigma}}_B = \mathbf{G}(\boldsymbol{\sigma}_B)\boldsymbol{\omega}_B \tag{10}$$

Suppose a reference motion is designed and, at the design stage, only the thrusters provide control torques, while the momentum wheels are non-rotating (*i.e.*, $\omega_{si} = 0, i = 1, 2, \cdots, N$). In this case, from Eq. (3), $\mathbf{h}_B = \mathbf{I}\boldsymbol{\omega}_B$. With the reference frame denoted by $\mathbf{R}$, the reference motion is assumed to be

$$\dot{\mathbf{h}}_R = \mathbf{h}_R^{\times}\mathbf{I}^{-1}\mathbf{h}_R + \mathbf{g}_R \tag{11}$$

where $\mathbf{h}_R = \mathbf{I}\boldsymbol{\omega}_R$ and $\boldsymbol{\omega}_R$ is the angular velocity of the virtual body in frame $\mathbf{R}$. Note that if the wheels are non-rotating and $\mathbf{g}_e = \mathbf{g}_R$ then Eqs. (1) and (11) are identical.

Thus, Eq. (11) describes the dynamics of the attitude motion of a "virtual" spacecraft with the same inertia properties as the real spacecraft. This virtual spacecraft is used to generate the desired (nominal or optimal) trajectory to be tracked. Hence, $\mathbf{g}_R$ in Eq. (11) is the desired nominal control torque which, if applied to the *real* spacecraft with the same initial conditions and with the wheels fixed with respect to the platform, would generate the desired trajectory.

The kinematics of frame $\mathbf{R}$ is given by

$$\dot{\boldsymbol{\sigma}}_R = \mathbf{G}(\boldsymbol{\sigma}_R)\boldsymbol{\omega}_R \tag{12}$$

where $\boldsymbol{\sigma}_R$ denote the MRPs of frame $\mathbf{R}$ with respect to the inertial frame $\mathbf{N}$.

We define the tracking error of the angular velocity expressed in frame $\mathbf{B}$ as

$$\delta\boldsymbol{\omega} = \boldsymbol{\omega}_B - \mathbf{C}_R^B\left(\delta\boldsymbol{\sigma}\right)\boldsymbol{\omega}_R \tag{13}$$

where $\mathbf{C}_R^B(\delta\boldsymbol{\sigma})$ is the rotation matrix from the reference frame $\mathbf{R}$ to the body frame $\mathbf{B}$, and $\delta\boldsymbol{\sigma}$ is the kinematics error between frames $\mathbf{B}$ and $\mathbf{R}$ defined by

$$\mathbf{C}_R^B(\delta\boldsymbol{\sigma}) = \mathbf{C}_N^B(\boldsymbol{\sigma}_B)\mathbf{C}_N^R(\boldsymbol{\sigma}_R)^T \tag{14}$$

From Eqs. (8) and (13), the differential equation for the error kinematics takes the form

$$\delta\dot{\boldsymbol{\sigma}} = \mathbf{G}(\delta\boldsymbol{\sigma})\delta\boldsymbol{\omega} \tag{15}$$

From Eq. (11), we have

$$\dot{\boldsymbol{\omega}}_R = \mathbf{I}^{-1}\mathbf{h}_R^{\times}\mathbf{I}^{-1}\mathbf{h}_R + \mathbf{I}^{-1}\mathbf{g}_R \tag{16}$$

thus

$$\mathbf{J}\mathbf{C}_R^B(\delta\boldsymbol{\sigma})\dot{\boldsymbol{\omega}}_R = \mathbf{J}\mathbf{C}_R^B(\delta\boldsymbol{\sigma})\mathbf{I}^{-1}\mathbf{h}_R^{\times}\mathbf{I}^{-1}\mathbf{h}_R + \mathbf{J}\mathbf{C}_R^B(\delta\boldsymbol{\sigma})\mathbf{I}^{-1}\mathbf{g}_R \tag{17}$$

According to the definition of the tracking error of the angular velocity in Eq. (13), we define the tracking error of the angular momentum expressed in frame **B** as

$$\begin{aligned}
\delta\mathbf{h} &= \mathbf{h}_B - \mathbf{J}\mathbf{C}_R^B(\delta\boldsymbol{\sigma})\boldsymbol{\omega}_R \\
&= \mathbf{I}\boldsymbol{\omega}_B + \mathbf{A}\mathbf{I}_s\boldsymbol{\omega}_s - \mathbf{J}\mathbf{C}_R^B(\delta\boldsymbol{\sigma})\boldsymbol{\omega}_R \\
&= \mathbf{J}(\boldsymbol{\omega}_B - \mathbf{C}_R^B(\delta\boldsymbol{\sigma})\boldsymbol{\omega}_R) \\
&\quad +\mathbf{A}(\mathbf{I}_s\boldsymbol{\omega}_s + \mathbf{I}_s A^T\boldsymbol{\omega}_B)
\end{aligned} \tag{18}$$

and using Eq. (6) we find that

$$\delta\mathbf{h} = \mathbf{J}\delta\boldsymbol{\omega} + \mathbf{A}\mathbf{h}_a \tag{19}$$

From Eq. (18) we develop the error dynamics as

$$\begin{aligned}
\delta\dot{\mathbf{h}} &= \dot{\mathbf{h}}_B - \mathbf{J}\frac{d\mathbf{C}_R^B(\delta\boldsymbol{\sigma})}{dt}\boldsymbol{\omega}_R - \mathbf{J}\mathbf{C}_R^B(\delta\boldsymbol{\sigma})\dot{\boldsymbol{\omega}}_R \\
&= \dot{\mathbf{h}}_B - \mathbf{J}\boldsymbol{\omega}_B^{\times}\delta\boldsymbol{\omega} - \mathbf{J}\mathbf{C}_R^B(\delta\boldsymbol{\sigma})\dot{\boldsymbol{\omega}}_R \\
&= \mathbf{h}_B^{\times}\mathbf{J}^{-1}(\mathbf{h}_B - \mathbf{A}\mathbf{h}_a) + \mathbf{g}_e - \mathbf{J}\boldsymbol{\omega}_B^{\times}\delta\boldsymbol{\omega} \\
&\quad -\mathbf{J}\mathbf{C}_R^B(\delta\boldsymbol{\sigma})\dot{\boldsymbol{\omega}}_R
\end{aligned} \tag{20}$$

where $\mathbf{J}\mathbf{C}_R^B(\delta\boldsymbol{\sigma})\dot{\boldsymbol{\omega}}_R$ is given in Eq. (17). Here we have used the fact that

$$\frac{d\mathbf{C}_R^B(\delta\boldsymbol{\sigma})}{dt}\boldsymbol{\omega}_R = \boldsymbol{\omega}_B^{\times}\delta\boldsymbol{\omega} \tag{21}$$

We give a brief proof of this fact in the Appendix.

The objective of the control laws developed in the sequel is to make the error dynamics of $\delta\boldsymbol{\sigma}$ and $\delta\boldsymbol{\omega}$ vanish asymptotically.

Tracking Controllers

In this section, we develop a combined control scheme to track rigid spacecraft attitude motions using *both* thrusters and momentum wheels. The thrusters may act as the feedforward portion of the controller while the momentum wheels implement the feedback portion of the controller. Alternatively, in case the thrusters can generate continuous control profiles, one may choose to implement the feedforward plus the nonlinear feedback portion of the control law through the thrusters. In this case, the controller for the momentum wheels implements a linear feedback control law in terms of the angular velocity and attitude errors. Both of these implementation schemes globally asymptotically stabilize the tracking error.

Consider the following candidate Lyapunov function [2]

$$\begin{aligned} V &= \frac{1}{2}\delta\boldsymbol{\omega}^T\mathbf{K}\delta\boldsymbol{\omega} + 2k_2\ln(1+\delta\boldsymbol{\sigma}^T\delta\boldsymbol{\sigma}) \\ &= \frac{1}{2}(\delta\mathbf{h}-\mathbf{A}\mathbf{h}_a)^T\mathbf{J}^{-1}\mathbf{K}\mathbf{J}^{-1}(\delta\mathbf{h}-\mathbf{A}\mathbf{h}_a) \\ &\quad +2k_2\ln(1+\delta\boldsymbol{\sigma}^T\delta\boldsymbol{\sigma}) \end{aligned} \tag{22}$$

where $\mathbf{K} = \mathbf{K}^T > 0$, and $k_2 > 0$. This function is positive definite and radially unbounded [7] in terms of the tracking errors $\delta\boldsymbol{\omega}$ and $\delta\boldsymbol{\sigma}$. Calculation of the derivative of V along the error kinematics and dynamics, Eqs. (15) and (20), yields

$$\dot{V} = (\delta\dot{\mathbf{h}}-\mathbf{A}\dot{\mathbf{h}}_a)^T\mathbf{J}^{-1}\mathbf{K}\mathbf{J}^{-1}(\delta\mathbf{h}-\mathbf{A}\mathbf{h}_a)$$

$$
\begin{aligned}
& +4k_2 \frac{\delta\boldsymbol{\sigma}^T \mathbf{G}(\delta\boldsymbol{\sigma})}{1+\delta\boldsymbol{\sigma}^T\delta\boldsymbol{\sigma}}\delta\boldsymbol{\omega} \\
= \; & (\delta\dot{\mathbf{h}} - \mathbf{A}\dot{\mathbf{h}}_a)^T \mathbf{J}^{-1}\mathbf{K}\delta\boldsymbol{\omega} + k_2\delta\boldsymbol{\sigma}^T\delta\boldsymbol{\omega} \qquad (23)
\end{aligned}
$$

Choosing $\mathbf{K} = \mathbf{J}$, we obtain

$$
\begin{aligned}
\dot{V} &= \delta\boldsymbol{\omega}^T(\delta\dot{\mathbf{h}} - \mathbf{A}\dot{\mathbf{h}}_a + k_2\delta\boldsymbol{\sigma}) \\
&= \delta\boldsymbol{\omega}^T \Big[\mathbf{h}_B^{\times}\mathbf{J}^{-1}(\mathbf{h}_B - \mathbf{A}\mathbf{h}_a) + \mathbf{g}_e - \mathbf{J}\boldsymbol{\omega}_B^{\times}\delta\boldsymbol{\omega} \\
&\quad -\mathbf{J}\mathbf{C}_R^B(\delta\boldsymbol{\sigma})\mathbf{I}^{-1}\mathbf{h}_R^{\times}\mathbf{I}^{-1}\mathbf{h}_R - \mathbf{J}\mathbf{C}_R^B(\delta\boldsymbol{\sigma})\mathbf{I}^{-1}\mathbf{g}_R \\
&\quad -\mathbf{A}\mathbf{g}_a + k_2\delta\boldsymbol{\sigma}] \qquad (24)
\end{aligned}
$$

We must select control torques $\mathbf{g}_a$ and $\mathbf{g}_e$ such that $\dot{V} < 0$ whenever $\delta\boldsymbol{\omega} \neq \mathbf{0}$ and $\delta\boldsymbol{\sigma} \neq \mathbf{0}$. Clearly there may be many possibilities, and in the next three subsections, we develop three different controllers based on Eq. (24).

Controller I

In case the thrusters are of the on-off type, they may not be able to implement a continuously varying control profile (unless a pulse-width pulse-modulation scheme is used) and thus, we assume that $\mathbf{g}_R$ is a bang-bang command. In this case we choose the thrusters to perform the designed nominal control $\mathbf{g}_R$; *i.e.*,

$$
\mathbf{g}_e = \mathbf{g}_R \qquad (25)
$$

and the momentum wheels are used to correct for the tracking errors. The nominal control, $\mathbf{g}_R$ is computed off-line using EZopt.

From Eq. (24), letting the feedback control law for the momentum wheels satisfy

$$\begin{aligned}\mathbf{A}\mathbf{g}_a &= \mathbf{h}_B^{\times}\mathbf{J}^{-1}(\mathbf{h}_B - \mathbf{A}\mathbf{h}_a) + \mathbf{g}_R - \mathbf{J}\boldsymbol{\omega}_B^{\times}\delta\boldsymbol{\omega} \\ &\quad -\mathbf{J}\mathbf{C}_R^B(\delta\boldsymbol{\sigma})\mathbf{I}^{-1}\mathbf{h}_R^{\times}\mathbf{I}^{-1}\mathbf{h}_R - \mathbf{J}\mathbf{C}_R^B(\delta\boldsymbol{\sigma})\mathbf{I}^{-1}\mathbf{g}_R \\ &\quad +k_1\delta\boldsymbol{\omega} + k_2\delta\boldsymbol{\sigma} \end{aligned} \tag{26}$$

yields

$$\dot{V} = -k_1\delta\boldsymbol{\omega}^T\delta\boldsymbol{\omega} \leq 0 \tag{27}$$

where $k_1 > 0$. This result implies that the tracking trajectories are bounded and furthermore,

$$\lim_{t\to\infty} \delta\boldsymbol{\omega}(t) = 0 \tag{28}$$

From Eqs. (19), (20) and (26), we have

$$\begin{aligned}\mathbf{J}\delta\dot{\boldsymbol{\omega}} &= \delta\dot{\mathbf{h}} - \mathbf{A}\dot{\mathbf{h}}_a \\ &= -k_1\delta\boldsymbol{\omega} - k_2\delta\boldsymbol{\sigma} \end{aligned} \tag{29}$$

Thus,

$$\lim_{t\to\infty} \mathbf{J}\,\delta\dot{\boldsymbol{\omega}} = -k_2 \lim_{t\to\infty} \delta\boldsymbol{\sigma}. \tag{30}$$

Because $\lim_{t\to\infty} \delta\boldsymbol{\omega} = 0$, we conclude that $\lim_{t\to\infty} \delta\boldsymbol{\sigma}$ cannot be a constant except zero. However, from Eqs. (15) and (28), $\lim_{t\to\infty} \delta\dot{\boldsymbol{\sigma}} = 0$. Hence $\lim_{t\to\infty} \delta\boldsymbol{\sigma}$ is a constant. Therefore,

$$\lim_{t\to\infty} \delta\boldsymbol{\sigma} = 0. \tag{31}$$

From LaSalle's Theorem [7], the tracking error dynamics and kinematics with the feedback control law (26) are shown to be globally asymptotically stable.

In the absence of any initial condition errors, *i.e.*, $\delta\boldsymbol{\omega}(0) = \delta\boldsymbol{\sigma}(0) = 0$, the control law in Eqs. (25) and (26) ensures perfect tracking; *i.e.*, $\boldsymbol{\omega}_B(t) = \boldsymbol{\omega}_R(t)$ and $\boldsymbol{\sigma}_B(t) = \boldsymbol{\sigma}_R(t)$ for all $t \geq 0$.

Controller II

Equations (25) and (26) show that Controller I is such that if initially $\boldsymbol{\omega}_B(0) = \boldsymbol{\omega}_R(0)$ and $\boldsymbol{\sigma}_B(0) = \boldsymbol{\sigma}_R(0)$ and, in addition, $\boldsymbol{\omega}_s(0) = 0$, then $\mathbf{h}_B(t) = \mathbf{h}_R(t)$ for all $t \geq 0$. In particular, the equality $\mathbf{h}_B(t) = \mathbf{h}_R(t)$ implies that $\mathbf{A}\mathbf{I}_s\boldsymbol{\omega}_s(t) = 0$ for all $t \geq 0$ and the momentum wheels can be commanded to remain stationary with respect to the platform.

An alternative control implementation is to choose the control law so that, in the absence of initial condition errors, and if the total axial rotor momentum is initially zero, $\mathbf{h}_a(0) = 0$, then it remains zero during the maneuver; *i.e.*, $\mathbf{h}_a(t) = 0$ for all $t \geq 0$. In this case, $\mathbf{h}_B = \mathbf{J}\boldsymbol{\omega}_B$ and we can therefore assume that the reference dynamics is given by

$$\dot{\mathbf{h}}_R = \mathbf{h}_R^{\times}\mathbf{J}^{-1}\mathbf{h}_R + \mathbf{g}_R \tag{32}$$

where $\mathbf{h}_R = \mathbf{J}\boldsymbol{\omega}_R$. Choosing the same Lyapunov function, the thruster control law as

$$\mathbf{g}_e = \mathbf{J}\mathbf{C}_R^B(\delta\boldsymbol{\sigma})\mathbf{J}^{-1}\mathbf{g}_R \tag{33}$$

and the momentum wheel control law

$$\begin{aligned}\mathbf{A}\mathbf{g}_a &= \mathbf{h}_B^{\times}\mathbf{J}^{-1}(\mathbf{h}_B - \mathbf{A}\mathbf{h}_a) - \mathbf{J}\boldsymbol{\omega}_B^{\times}\delta\boldsymbol{\omega} \\ &\quad -\mathbf{J}\mathbf{C}_R^B(\delta\boldsymbol{\sigma})\mathbf{J}^{-1}\mathbf{h}_R^{\times}\mathbf{J}^{-1}\mathbf{h}_R \\ &\quad +k_1\delta\boldsymbol{\omega} + k_2\delta\boldsymbol{\sigma} \end{aligned} \tag{34}$$

we obtain Eq. (27). This control leads to the same expression for $\dot{V}$ as in Controller I. Therefore, using similar arguments as for Controller I, one can show that this control law achieves global asymptotic stability for the tracking error dynamics.

Note that in the absence of any initial condition errors, $\delta\boldsymbol{\sigma}(0) = \delta\boldsymbol{\omega}(0) = 0$, and if $\mathbf{h}_a(0) = 0$, the control law in Eqs. (33) and (34) guarantees that $\delta\boldsymbol{\sigma}(t) = \delta\boldsymbol{\omega}(t) = 0$ for all $t \geq 0$ and the control law becomes

$$\mathbf{g}_e = \mathbf{g}_R \tag{35}$$

and

$$\mathbf{A}\mathbf{g}_a = \mathbf{h}_B^{\times}\mathbf{J}^{-1}(\mathbf{h}_B - \mathbf{A}\mathbf{h}_a) - \mathbf{h}_R^{\times}\mathbf{J}^{-1}\mathbf{h}_R = (\mathbf{A}\mathbf{h}_a)^{\times}\boldsymbol{\omega}_R \tag{36}$$

The last equation, along with Eq. (2) implies that if $\mathbf{h}_a(0) = 0$, then $\mathbf{g}_a = 0$ and hence, $\mathbf{h}_a(t) = 0$, for all $t \geq 0$.

Controller III

An alternative way to implement the control law is to enforce a linear feedback control law for the wheels:

$$\mathbf{A}\mathbf{g}_a = k_1\delta\boldsymbol{\omega} + k_2\delta\boldsymbol{\sigma} \tag{37}$$

Then one needs to choose the thruster control law as

$$\mathbf{g}_e = -\mathbf{h}_B^{\times}\mathbf{J}^{-1}(\mathbf{h}_B - \mathbf{A}\mathbf{h}_a) + \mathbf{J}\boldsymbol{\omega}_B^{\times}\delta\boldsymbol{\omega} + \mathbf{J}\mathbf{C}_R^B(\delta\boldsymbol{\sigma})\dot{\boldsymbol{\omega}}_R \tag{38}$$

where $\dot{\boldsymbol{\omega}}_R$ is given either from Eq. (11) or from Eq. (32). In the first case, we have $\mathbf{h}_R = \mathbf{I}\boldsymbol{\omega}_R$ whereas in the second case we have $\mathbf{h}_R = \mathbf{J}\boldsymbol{\omega}_R$.

The Lyapunov function in Eq. (22) can be used to show that this control law renders the error system $(\delta\boldsymbol{\omega}, \delta\boldsymbol{\sigma})$ globally asymptotically stable, again with the same expression for $\dot{V}$ as in the previous two controllers.

Remark: A word of caution in the implementation of the previous controllers should be mentioned at this point. Since the MRPs used for the attitude kinematics define a three-dimensional set of parameters, they will encounter a singular orientation, which for the MRPs case is at an eigenaxis rotation of 360°. When describing the attitude error $\delta\boldsymbol{\sigma}$ this singularity does not create any problems, since closed-loop stability subsumes existence of solutions for all $t \geq 0$. Hence the attitude error cannot have finite escape times (see Ref. [7]). For the general tracking case, however, the reference attitude could easily exceed $\Phi = 360\,\text{deg}$. In such a case, one can then use the dual or shadow set of MRPs [5] to by-pass any attitude singularities. One of the nice features of the dual set is that they obey the same differential equation, (8–9). Therefore, their use merely amounts to "resetting" the attitude state whenever the parameters leave their region of validity; for details see Refs. [2, 5]. Alternatively, a non-singular global set, such as the Euler parameters, can be used for the reference and actual attitude descriptions, while still using the MRPs for the attitude error.

The control laws proposed in this paper will still remain the same in this case, modulo a transformation of the reference and actual attitude from the Euler parameter set to the MRP set.

Numerical Examples

To illustrate the effectiveness of these control laws, we apply them to track a trajectory of a minimum-time rest-to-rest maneuver. Three momentum wheels are used to provide the feedback control. They are aligned with the principal axes and their axial moments of inertia are given by $\mathbf{I}_s = \text{diag}\{0.01, 0.01, 0.01\}\,\text{kg}\,\text{m}^2$. The spacecraft moment of inertia matrix is $\mathbf{I} = \text{diag}\,\{200, 150, 175\}\ \text{kg}\,\text{m}^2$. The nominal control $\mathbf{g}_R$, which is known to be bang-bang [1], is designed to drive the spacecraft from an initial attitude, $\boldsymbol{\sigma}_R(0) = (0.10, 0.20, 0.30)$, which can be represented in 3-2-1 Euler angles as $(42°, 20°, 78°)$, to a position aligned with the inertial frame; *i.e.*, $\boldsymbol{\sigma}(t_f) = (0, 0, 0)$. We assume that the actual initial attitude of the body frame is $\boldsymbol{\sigma}_B(0) = (0.11, 0.15, 0.28)$, which can be expressed in 3-2-1 Euler angles as $(37°, 13°, 69°)$.

We present results for all three controllers in Figs. 1–7. In all cases, the gains are $k_1 = 54$ and $k_2 = 47$. These gains are selected so that all three controllers provide performance which is similar to that provided by the ideal bang-bang control with no initial condition errors. We compute the bang-bang control thrust profiles off-line using the EZopt Optimal Control Toolkit [8]. In practice, a real-time approach for computing the reference thrust profiles would be required.

Figure 1 shows the time histories of $\delta\boldsymbol{\omega}$ and $\delta\boldsymbol{\sigma}$ for all three controllers, which

are identical. The plots in Fig. 1 show that the angular velocity and attitude errors are driven asymptotically to zero. Figures 2 and 3 show the time history of the controls when the thrusters perform the nominal bang-bang control $\mathbf{g}_R$ and the control law for the momentum wheels is given by Eq. (26); *i.e.*, Controller I is used. The thrusters provide the ideal time-optimal control, while the momentum wheels provide the piecewise smooth torques to eliminate tracking errors caused by the initial condition errors.

Figures 4 and 6 illustrate the time history of the control inputs for Controller II, where the thrusters perform the control law in Eq. (33) and the momentum wheels perform the linear feedback control law in Eq. (34), with reference input generated by Eq. (32). The thruster torque profile is similar, but not identical, to the bang-bang control shown in Fig. 2. The differences are due to the attitude error feedback that is incorporated into Eq. (33). Since the thruster torque profile is similar to the bang-bang control of Fig. 2, in Fig. 4 we plot the difference between the actual torque and the reference torque; *i.e.*, we plot $\delta\mathbf{g}_e = \mathbf{g}_e - \mathbf{g}_R$.

Figures 5 and 7 illustrate the time history of the control inputs for Controller III, where the thrusters perform the control law in Eq. (38) and the momentum wheels perform the linear feedback control law in Eq. (37), with reference input generated by Eq. (11). These controls are similar to those for Controller II. As in Fig. 4, Fig. 5 shows the difference between the actual torque and the reference torque. Note also that the momentum wheel controls for Controllers II and III are smooth, in contrast

with the momentum wheel control for Controller I. However, the disadvantage of Controllers II and III is that the thrusters must provide variable thrust levels.

Conclusions

Control laws are developed to combine the external and internal torques provided by thrusters and momentum wheels for tracking prescribed large-angle rotational maneuvers. The control laws are based on the nonlinear equations of motion for the spacecraft angular momentum and the modified Rodrigues parameters, and are designed to be globally asymptotically stable in tracking prescribed rigid body maneuvers. Since thrusters generally are not capable of providing continuously varying torques, one approach to rotational maneuvers is to use the thrusters for bang-bang control to provide the coarse maneuver, and to use the momentum wheels as continuous controllers to provide the necessary corrections. In case the thrusters are capable of providing continuously varying torques, alternative control laws can be used, including one in which the wheel torque control is linear.

Appendix

Here we give a brief proof of Eq. (21). It is well known in analytical dynamics [9] that

$$\dot{\mathbf{C}}_N^B = -\boldsymbol{\omega}_B^\times \mathbf{C}_N^B, \text{ and } \dot{\mathbf{C}}_N^R = -\boldsymbol{\omega}_R^\times \mathbf{C}_N^R \tag{39}$$

so

$$\frac{d\mathbf{C}_R^B}{dt} = \frac{d[\mathbf{C}_N^B \mathbf{C}_R^N]}{dt}$$

$$
\begin{aligned}
&= \dot{\mathbf{C}}_N^B \mathbf{C}_R^N + \mathbf{C}_N^B \dot{\mathbf{C}}_R^N \\
&= -\boldsymbol{\omega}_B^\times \mathbf{C}_N^B \mathbf{C}_R^N + \mathbf{C}_N^B [-\boldsymbol{\omega}_R^\times \mathbf{C}_N^R]^T \\
&= -\boldsymbol{\omega}_B^\times \mathbf{C}_N^B \mathbf{C}_R^N + \mathbf{C}_N^B [-\boldsymbol{\omega}_R^\times \mathbf{C}_B^R \mathbf{C}_N^B]^T \\
&= -\boldsymbol{\omega}_B^\times \mathbf{C}_N^B \mathbf{C}_R^N + \mathbf{C}_N^B [\mathbf{C}_N^B]^T \mathbf{C}_R^B \boldsymbol{\omega}_R^\times \\
&= -\boldsymbol{\omega}_B^\times \mathbf{C}_R^B + \mathbf{C}_R^B \boldsymbol{\omega}_R^\times \qquad (40)
\end{aligned}
$$

Thus

$$
\begin{aligned}
\frac{d\mathbf{C}_R^B}{dt}\boldsymbol{\omega}_R &= -\boldsymbol{\omega}_B^\times \mathbf{C}_R^B \boldsymbol{\omega}_R \\
&= -\boldsymbol{\omega}_B^\times [\boldsymbol{\omega}_B - \delta\boldsymbol{\omega}] \\
&= \boldsymbol{\omega}_B^\times \delta\boldsymbol{\omega} \qquad (41)
\end{aligned}
$$

which concludes the proof.

Acknowledgements

The work of the first author was supported in part by AFOSR award: F49620-01-1-0106 and NSF award: CMS-9978745. The work of the last two authors was supported in part by AFOSR award: F49620-00-1-0374 and NSF award: CMS-9996120.

References

[1] JUNKINS, J. L. and TURNER, J. D., *Optimal Spacecraft Rotational Maneuvers*, Vol. 3 of *Studies in Astronautics*, Elsevier Science Publishers, Amsterdam, 1986.

[2] TSIOTRAS, P., "Stabilization and Optimality Results for the Attitude Control Problem," *Journal of Guidance, Control and Dynamics*, Vol. 19, No. 4, 1996, pp. 772–777.

[3] HALL, C. D., "Momentum Transfer in Two-Rotor Gyrostats," *Journal of Guidance, Control and Dynamics*, Vol. 19, No. 5, 1996, pp. 1157–1161.

[4] TSIOTRAS, P., SHEN, H., and HALL, C. D., "Satellite Attitude Control and Power Tracking with Energy/Momentum Wheels," *Journal of Guidance, Control and Dynamics*, Vol. 24, No. 1, 2001, pp. 23–34.

[5] SCHAUB, H. and JUNKINS, J. L., "Stereographic Orientation Parameters for Attitude Dynamics: A Generalization of the Rodrigues Parameters," *Journal of the Astronautical Sciences*, Vol. 44, No. 1, 1996, pp. 1–20.

[6] SCHAUB, H., ROBINETT, R. D., and JUNKINS, J. L., "Globally Stable Feedback Laws for Near-Minimum-Fuel and Near-Minimum-Time Pointing Maneuvers for a Landmark-Tracking Spacecraft," *Journal of the Astronautical Sciences*, Vol. 44, No. 4, 1996, pp. 443–466.

[7] KHALIL, H. K., *Nonlinear Systems*, Macmillan, New York, 1992.

[8] ANALYTICAL MECHANICS ASSOCIATES, *EZopt: An Optimal Control Toolkit*, Hampton, Virginia, 1999.

[9] HUGHES, P. C., *Spacecraft Attitude Dynamics*, John Wiley & Sons, New York, 1986.

Figure Captions

Fig. 1. Time histories of $\delta\boldsymbol{\omega}$ and $\delta\boldsymbol{\sigma}$ for all three controllers

Fig. 2. Nominal bang-bang control performed by thrusters for Controller I

Fig. 3. Feedback control performed by momentum wheels for Controller I

Fig. 4. Difference between control performed by thrusters for Controller II and the reference torque

Fig. 5. Difference between control performed by thrusters for Controller III and the reference torque

Fig. 6. Feedback control performed by momentum wheels for Controller II

Fig. 7. Feedback control performed by momentum wheels for Controller III

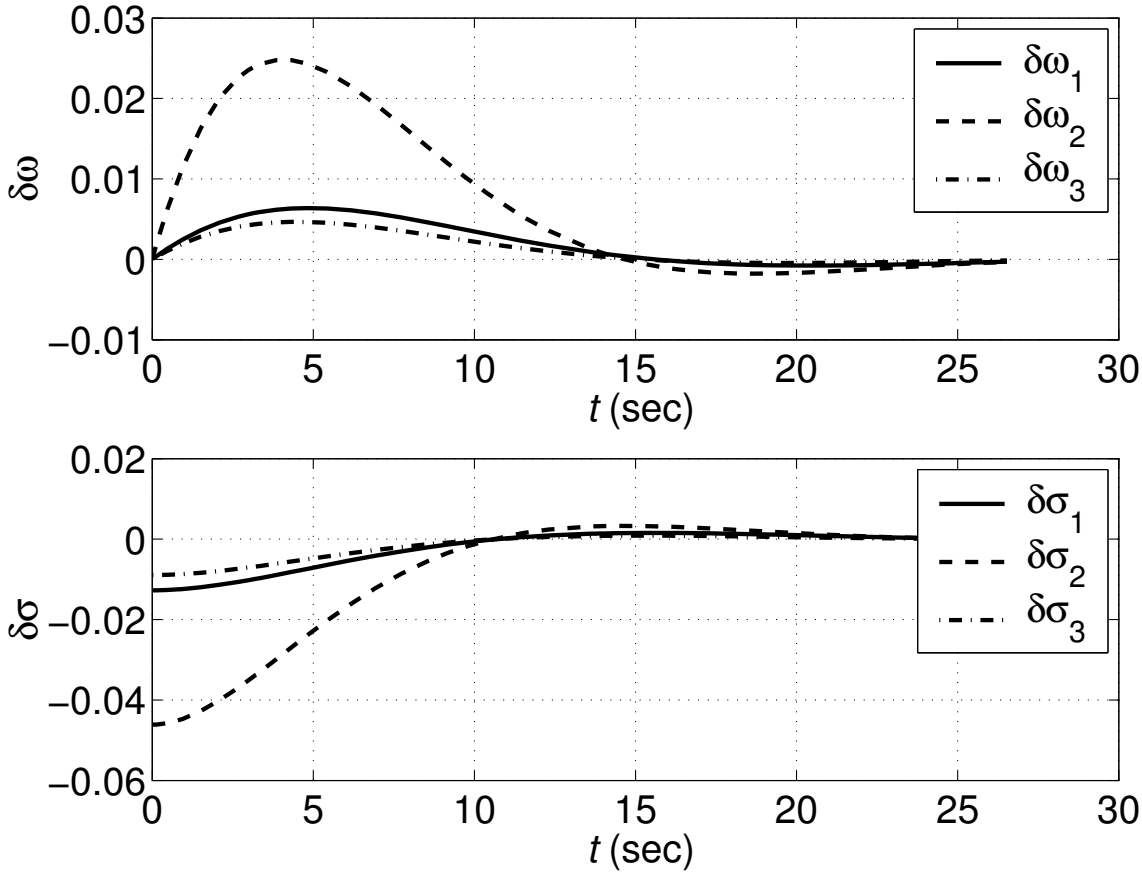

Figure 1: Time histories of $\delta\boldsymbol{\omega}$ and $\delta\boldsymbol{\sigma}$ for all three controllers

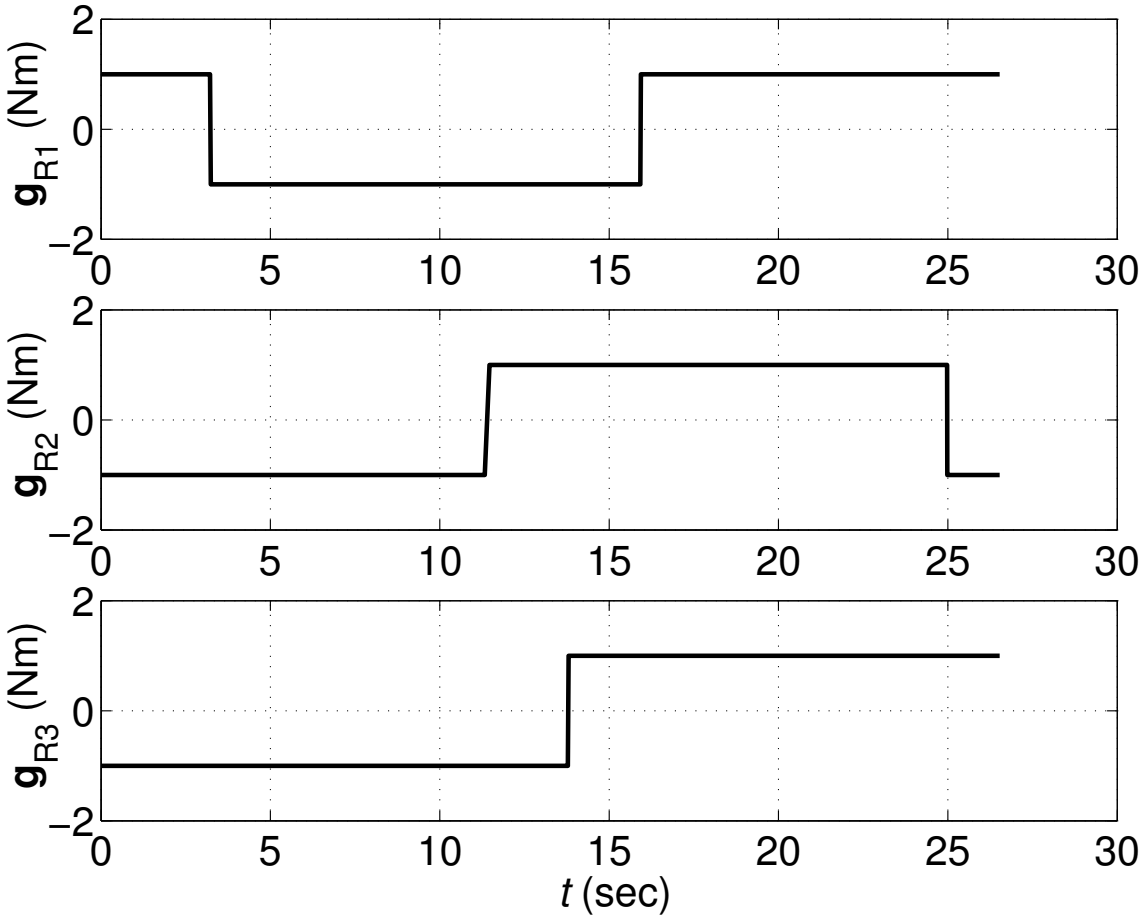

Figure 2: Nominal bang-bang control performed by thrusters for Controller I

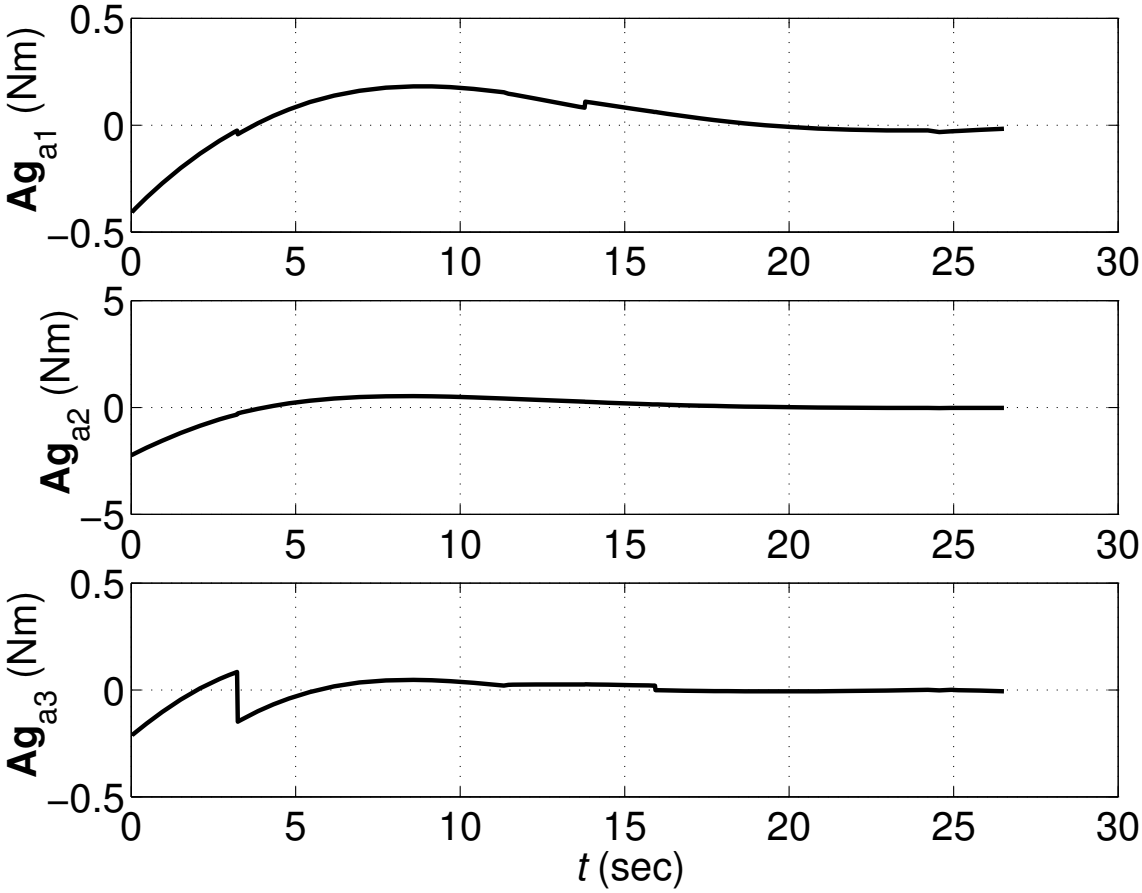

Figure 3: Feedback control performed by momentum wheels for Controller I

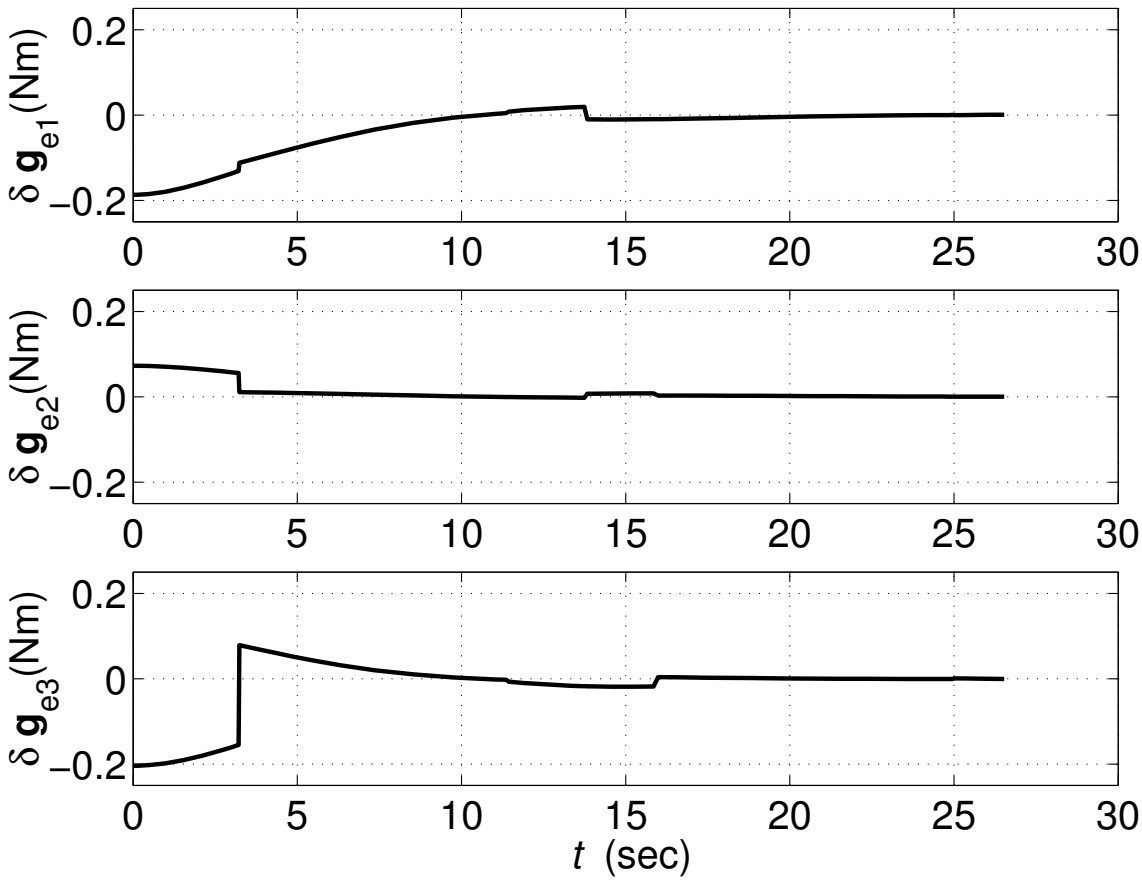

Figure 4: Difference between control performed by thrusters for Controller II and the reference torque

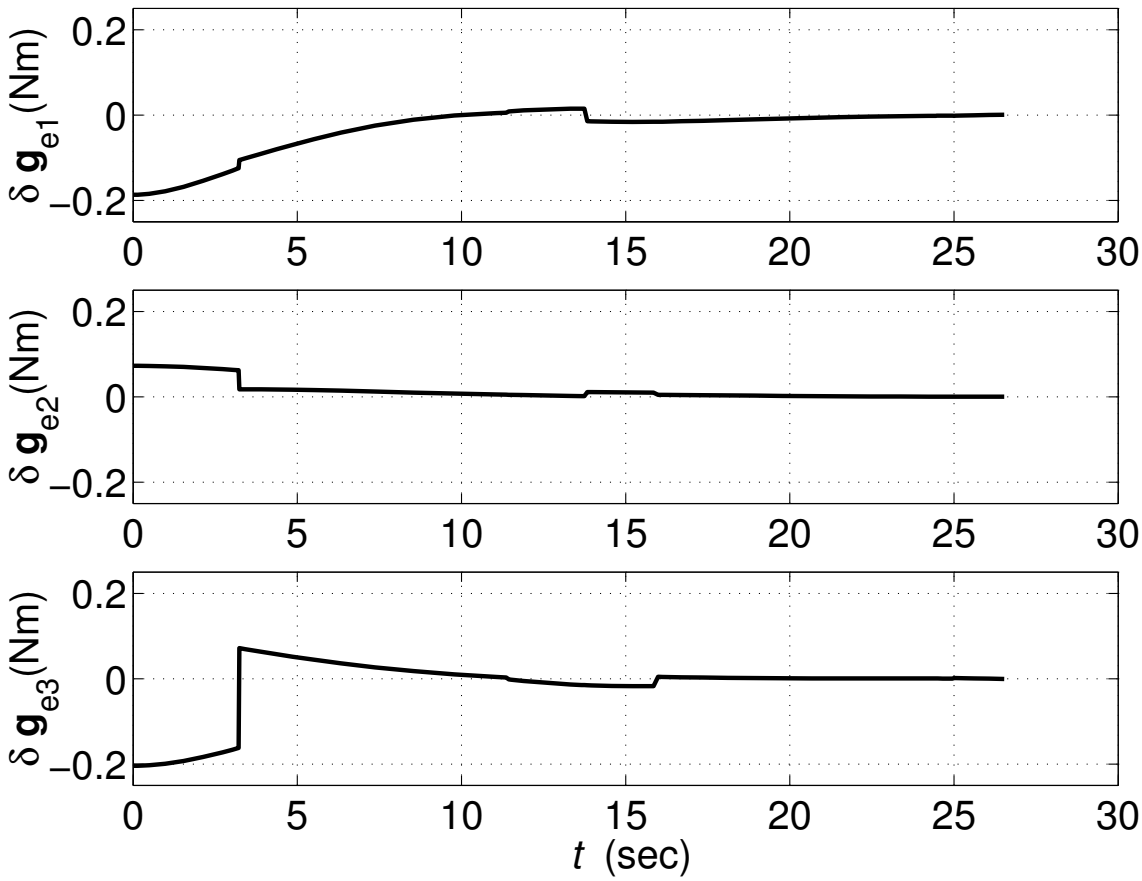

Figure 5: Difference between control performed by thrusters for Controller III and the reference torque

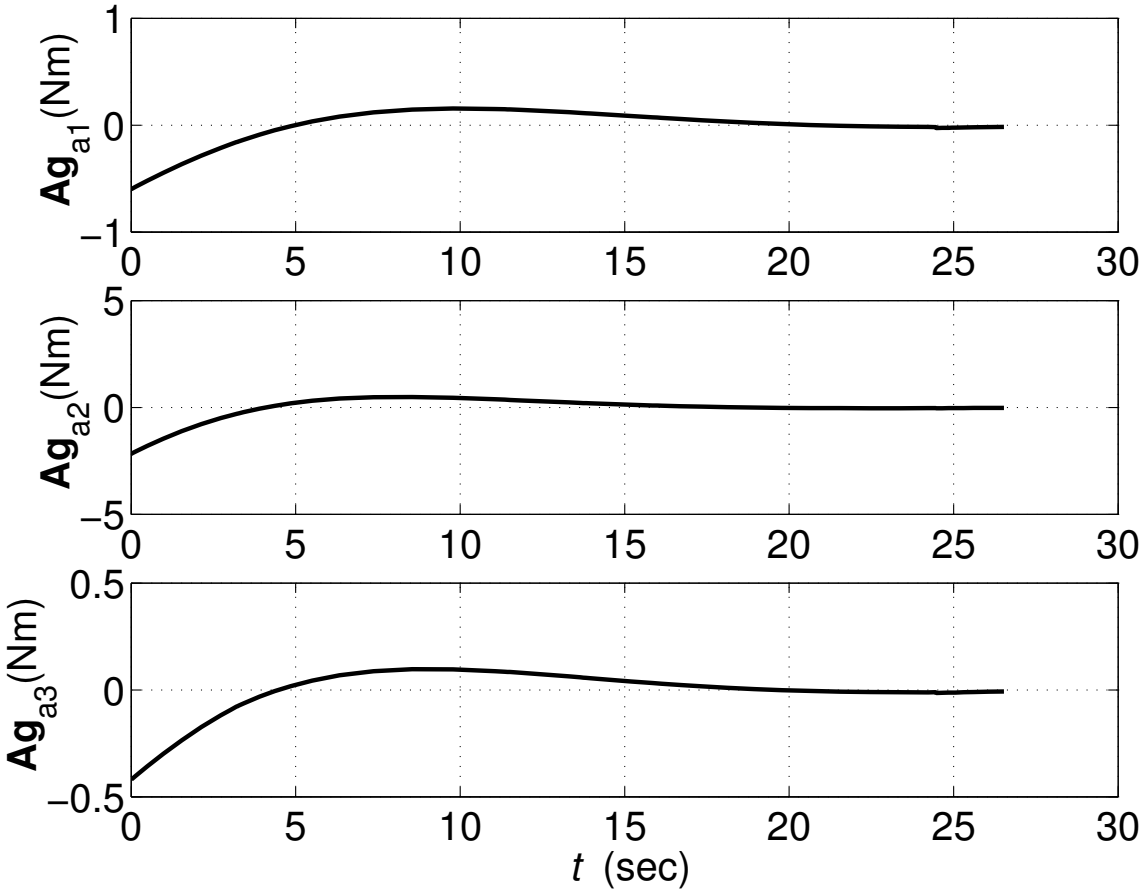

Figure 6: Feedback control performed by momentum wheels for Controller II

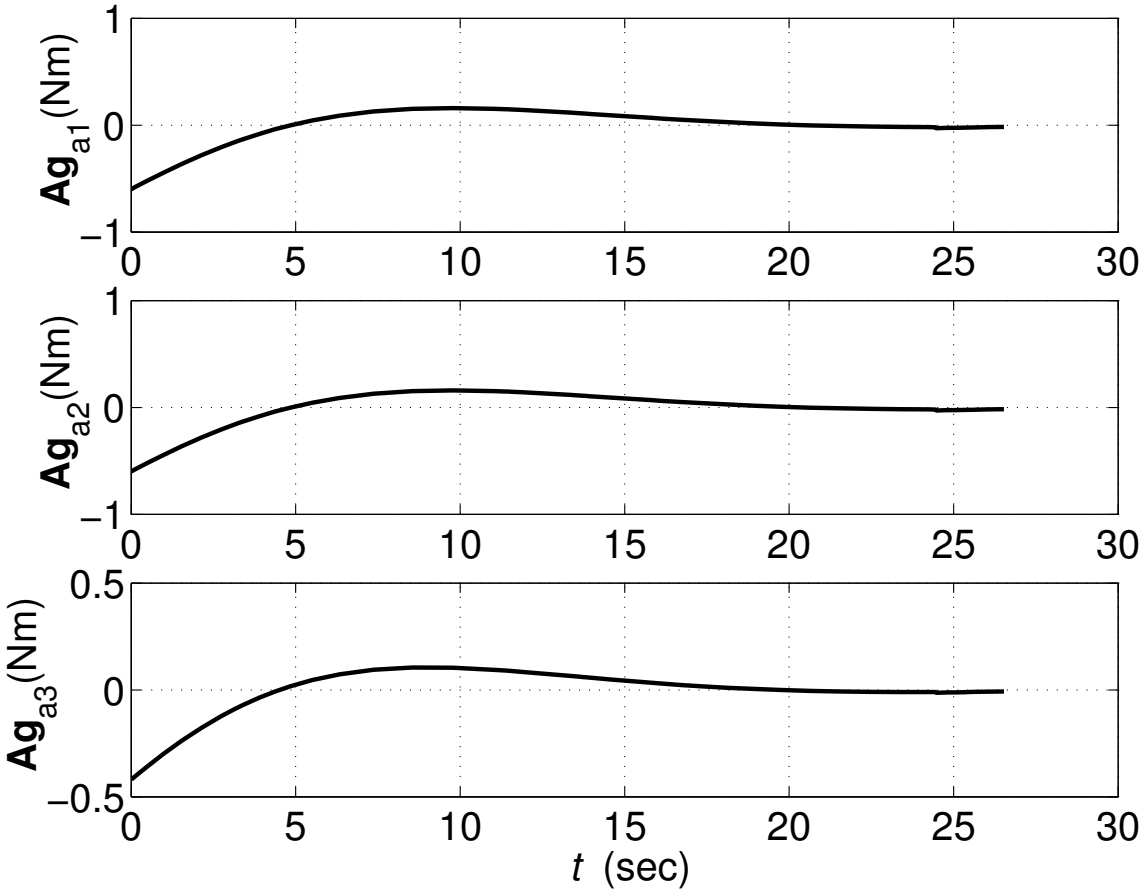

Figure 7: Feedback control performed by momentum wheels for Controller III